MOLECULAR PLANT PATHOLOGY (2009) **10**(2), 223–236 DOI: 10.1111/J.1364-3703.2008.00524.X

A proteomic analysis of powdery mildew (*Blumeria graminis* f.sp. *hordei*) conidiospores

SANDRA NOIR, THOMAS COLBY, ANNE HARZEN, JÜRGEN SCHMIDT AND RALPH PANSTRUGA*

Max-Planck-Institute for Plant Breeding Research, Carl-von-Linné-Weg 10, D-50829 Cologne, Germany

SUMMARY

Conidiospores are the asexual propagation units of many plant-pathogenic fungi. In this article, we report an annotated proteome map of ungerminated conidiospores of the ascomycete barley powdery mildew pathogen, *Blumeria graminis* f.sp. *hordei*. Using a combination of two-dimensional polyacrylamide gel electrophoresis and matrix-assisted laser desorption ionization-time-of-flight mass spectrometry, we have identified the proteins in 180 spots, which probably represent at least 123 distinct fungal gene products. Most of the identified proteins have a predicted function in carbohydrate, lipid or protein metabolism, indicating that the spore is equipped for the catabolism of storage compounds as well as for protein biosynthesis and folding on germination.

INTRODUCTION

Blumeria graminis f.sp. *hordei* (*Bgh*) is the causal agent of powdery mildew in barley (Collins *et al.*, 2002). It is one of the major diseases affecting this monocotyledonous plant species, leading to a decrease in yield and quality in barley agriculture. *Bgh* is one of the most intensively studied powdery mildew fungi and, like all species of the Erysiphales (powdery mildews), it is an obligate biotrophic pathogen, requiring a living plant host for growth and propagation (Both and Spanu, 2004). Initial events in the asexual life cycle of the fungus comprise spore germination, appressorium formation (Fig. 1A), host cell penetration and the intracellular establishment of its feeding organ, the so-called haustorium (Green *et al.*, 2002). Following successful host cell entry, the fungal mycelium proliferates on the leaf surface and, from about 5 days post-inoculation onwards, numerous spore carriers (conidiophores) emerge to produce large quantities of asexual conidia that are spread to other host plants via the wind (Fig. 1B; Green *et al.*, 2002).

* *Correspondence*: Tel.: +49 221 5062 316; Fax: +49 221 5062 353; E-mail: panstrug@mpiz-koeln.mpg.de

Despite the extensive research carried out on the barley powdery mildew pathogen, the basic molecular biology of *Bgh* remains poorly understood (Zhang *et al.*, 2005). Its obligate biotrophic lifestyle and our current inability to cultivate the fungus *in vitro* or effectively manipulate it genetically severely limit the experimental repertoire. Consequently, thorough experimental examination of the powdery mildews at the molecular level has lagged significantly behind that of other pathogenic fungi, in spite of their economic and agricultural importance. Only recently, two studies based on transcript profiling using cDNA microarrays comprising 2027 *Bgh* genes allowed new insights into *Bgh* biology. The first study focused on the determinants of pathogenicity (Both *et al.*, 2005b), revealing a global shift in gene expression between the pre- and post-penetrative stages of the fungus. In particular, genes encoding polypeptides related to protein biosynthesis exhibited a dramatic increase in transcript abundance, suggesting that the formation of post-penetrative infection structures and the establishment of a stable pathogenic relationship require high levels of *de novo* protein biosynthesis. The second analysis highlighted a striking degree of apparent co-expression of genes encoding enzymes of particular primary metabolic pathways. Although several genes encoding components of glycolysis were found to be coordinately up-regulated during appressorium formation, transcripts of enzymes involved in lipid catabolism were abundant in conidia and decreased at later developmental stages (Both *et al.*, 2005a).

To strengthen our knowledge about obligate biotrophic fungi, and to corroborate or complement transcriptome analyses, it is important to determine the protein equipment of these organisms at various developmental stages. Proteomic technologies, such as protein separation by two-dimensional gel electrophoresis and peptide analysis by mass spectrometry (MS), generally enable the efficient identification and characterization of proteins in filamentous fungi (for a review, see Kim *et al.*, 2007). Nevertheless, obligate biotrophs, such as powdery mildews, downy mildews and rust fungi, cannot be cultured extensively *in vitro*, thereby generally complicating proteomic studies. A lack of comprehensive cDNA data and an absence of partial or full

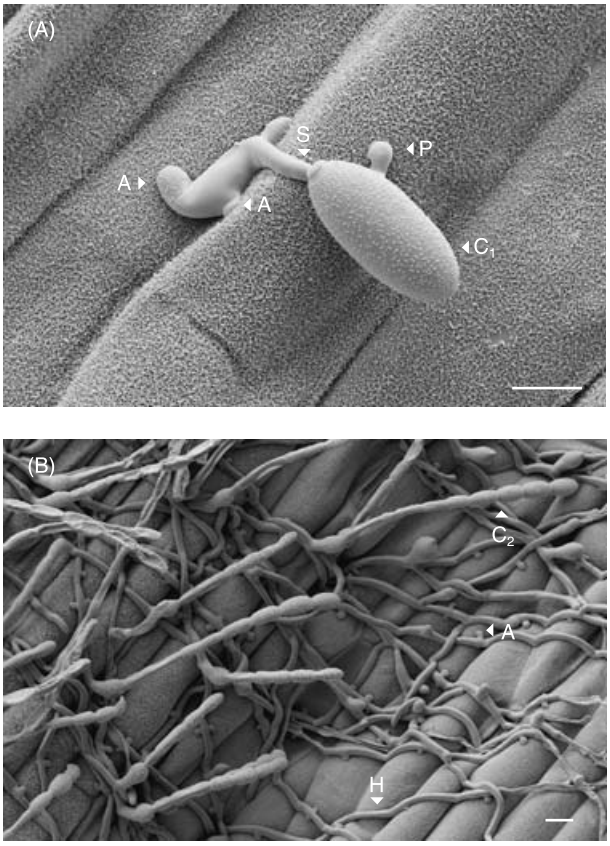

Fig. 1 Scanning electron micrographs of *Blumeria graminis* f.sp. *hordei* (*Bgh*) conidiophores and germinated conidia. The micrographs depict a germinated conidiospore on its host barley (A) (scale bar, 10 μm) and mature conidiophores bearing terminal strings of conidia (B) (scale bar, 20 μm). A, appressorium; C_1, conidium; C_2, conidiophore; H, hypha; P, primary germ tube; S, secondary germ tube. Pictures are courtesy of Sarah Maria Schmidt and Elmon Schmelzer.

genome sequences further hamper proteome profiling in most cases. Consequently, few proteomic surveys of obligate biotrophs have been reported to date (Cooper *et al.*, 2006, 2007; Rampitsch *et al.*, 2006).

The only period of development when powdery mildew fungi are free of any biotrophic relationship with their host is the conidium stage, enabling extensive analysis of this developmental phase. Conidia of powdery mildews are asexual, non-motile fungal spores that are dispersed by the wind. They are one-celled, uninucleate, vacuolated and thin-walled organisms (Braun *et al.*, 2002) that contain glycogen and abundant lipid droplets as storage compounds to fuel germination on contact with the host (Both *et al.*, 2005a; McKeen, 1970). *Bgh* conidia are produced in chains that are connected to the colony via upright spore carriers (conidiophores; Fig. 1B). The spores normally do not germinate as long as they are attached to the conidiophore, but they do so rapidly on separation. This physiological characterization suggests that conidia are not entirely passive, but that inhibitory processes suppress germination of spores attached to the mother colony (Green *et al.*, 2002). Further evidence for pre-germination conidial activity is provided by studies on the secretion of conidial extracellular material (ECM). This substance seems to be released from spores immediately on contact with the leaf surface. ECM exhibits hydrolytic enzyme activities and may contain preformed enzymes, such as esterases, lipases or hydrolases (Green *et al.*, 2002).

Little is known about the complex physiological changes that occur during fungal spore germination (Osherov and May, 2001). This, in particular, applies to conidia of fungal phytopathogens, which have only recently become the subject of detailed molecular analyses. Global transcript profiling of *Bgh* and *Fusarium graminearum* have revealed first snapshots of the changes in gene expression during the early developmental stages of fungal plant parasites (Both *et al.*, 2005a,b; Seong *et al.*, 2008). Reminiscent of the findings in *Bgh* (see above), the analysis of the *F. graminearum* transcriptome uncovered a major involvement of genes related to peroxisome biogenesis and fatty acid metabolism in ungerminated spores, whereas germinated spores showed a shift towards the expression of genes involved in metabolism and energy functions using carbon compounds and carbohydrates. In addition to genes related to this metabolic change, *F. graminearum* germinated spores exhibited elevated transcript levels of genes related to transcription and translation machineries, the cell cycle, cellular transport and cellular biogenesis (Seong *et al.*, 2008). At present, only a few proteomic studies have complemented these transcriptome analyses and have provided initial insights into the respective fungal protein equipment (Cooper *et al.*, 2006, 2007). Notably, however, the comparative proteomic analysis of ungerminated and germinated spores of the biotrophic bean rust fungus, *Uromyces appendiculatus*, revealed only a few significant differences between these two developmental stages, suggesting that the proteome of ungerminated fungal spores represents a valuable approximation of the protein inventory of germinated sporelings (Cooper *et al.*, 2006, 2007).

In this article, we report, to our knowledge, the first proteome analysis of a biotrophic powdery mildew fungus. We have focused on ungerminated asexual conidia, as these fungal structures can be readily collected and provide a homogeneous biological source material of high purity. By combining two-dimensional gel electrophoresis with matrix-assisted laser desorption ionization time-of-flight mass spectrometry (MALDI-TOF MS) and tandem time-of-flight mass spectrometry (MALDI-TOF/TOF MS/MS), we were able to determine the identity of 180 protein spots and to establish a functionally annotated reference proteome map for *Bgh* conidia.

RESULTS AND DISCUSSION

Establishment of a proteome map of *Bgh* conidia

Two batches of approximately 600 mg of fresh *Bgh* conidia were collected from approximately 200 barley plants that had been inoculated 7 days earlier. From each replicate, approximately 1–2 mg of total protein were extracted and purified by trichloroacetic acid precipitation and phenol extraction. Aliquots (approximately 160 μg from the first batch) of the purified protein samples were subjected to two-dimensional gel electrophoresis as described in 'Experimental procedures'; the second batch of samples was used as replicates. The samples were analysed in three different pI ranges (pI 3–10, 4–7 and 6–10) on colloidal Coomassie blue-stained gels (Fig. 2). Initially, 124 spots were cut out and analysed from the pI 3–10 range gel, 136 from the pI 4–7 range gel and 56 from the pI 6–11 range gel, adding up to a total of 316 excised spots (Fig. 3). Of these, 230 (116 from pI 3–10, 70 from pI 4–7 and 44 from pI 6–10) were identified by MS analysis as described below, giving rise to an overall identification rate of 73% (Fig. 3). As judged by manual inspection and comparison of the three gel types, 133 spots were identified from a gel in a single pI range, and 47 were identified from gels in multiple pI ranges (Fig. 4). This partial redundancy resulted in a final number of 180 distinct identified spots, represented by the entirety of 230 characterized spots from the three gel types (Figs 3 and 4). Owing to the two-dimensional gel electrophoresis separation procedure employed, these are expected to comprise predominantly soluble cytoplasmic proteins.

Protein identification

All protein spots were processed by automated in-gel tryptic digestion and MALDI-TOF MS analysis to generate peptide mass fingerprints (PMFs). Sequence information for selected peptides was then obtained from the samples by MALDI-TOF/TOF MS/MS using laser-induced dissociation (Suckau *et al.*, 2003). Co-migration of multiple proteins in two-dimensional gel electrophoresis was observed in the case of 10 of the 230 spots successfully analysed in this study. In each of these instances, two or three distinct polypeptides were identified by a combination of MALDI-TOF and TOF/TOF analysis (Fig. 2; Table 1). Initially, the spectra of 113 protein spots were directly assigned to at least one known protein (GI accession) by screening the National Center for Biotechnology Information non-redundant (NCBInr) database. This procedure revealed mostly hits from fungi other than *Bgh*, indicating that these polypeptides represent conserved fungal proteins (Table 1). The spectra of all spots were then searched against publicly available *Bgh* expressed sequence tags (NCBI ESTs) and the *Bgh* draft genome sequence (assembly from June 2007) kindly provided by P. Spanu and coworkers (Imperial College, London, UK; unpublished data) (http://www.blugen.org/). These searches revealed that more than one-half of the previously assigned spectra (73 of 113) also matched to *Bgh* ESTs and, furthermore, led to the identification of an additional 44 proteins based on *Bgh* ESTs and 23 proteins based on open reading frames (ORFs) predicted from *Bgh* genomic contigs (Supplement S1, see 'Supporting Information'). For the latter two modes of identification the corresponding translated sequences were used for BLAST searches against the NCBInr database (http://blast.ncbi.nlm.nih.gov/Blast.cgi) and the best hit was used to annotate the particular polypeptide (Tables 1 and S1, and Table S1 caption, see 'Supporting Information'). In total, 117 annotated proteins matched to *Bgh* ESTs (73 *Bgh* homologues of hits against the NCBInr database plus 44 'EST-only' hits), meaning that 63 (*c.* 35%) are proteins that are currently not represented by *Bgh* ESTs of sufficient length or quality (Fig. 3). This clearly underscores the value of investigations at the proteome level as a useful complement to transcriptome studies and/or genome annotation. The final annotation of the *Bgh* spore proteome (comprising 180 identified spots as described above) revealed a total of 174 spots with either direct or indirect hits to polypeptides, whereas six spots resulted in matches to *Bgh* ESTs with no counterpart in the protein databases (Table 1, spots 174–179). Of the 174 protein hits, 11 (6%) matched directly to published *Bgh* proteins, 153 (88%) corresponded to homologues from other fungal species and only 10 (6%) matched homologues of non-fungal organisms (e.g. plants, protists, bacteria and animals). The observed paucity of *Bgh*-derived protein hits is not surprising as only 51 *Bgh* polypeptide entries are currently (June 2008) present in the NCBInr database. It is conceivable that the proteins that do not match to fungal proteins result from organisms contaminating our biological source material.

Given the relatively poor number and completeness of publicly available *Bgh* sequences, most identifications presented in Tables 1/S1 were found on the basis of local homology by MS/MS searching. The comparatively low sequence coverage for most proteins reflects this limitation; many matches either represent homologues from other organisms or incomplete *Bgh* sequences (ESTs). As all sample spectra were searched against multiple public sequence resources, the best hit is reported in each case. Where identifications could only be achieved using ORFs of the *Bgh* draft genome, the sequences of the translated ORFs are available as a FASTA file in the Supporting Information (Supplement S1). In the light of these constraints, the current study focuses on the functional classification of the identified proteins, rather than their correlation to individual genes in an incomplete genome.

The identified proteins ranged in calculated molecular mass from 15.4 to 174 kDa, and in calculated pI from 4.6 to 11.3, thus encompassing a broad range of biophysical properties (Table 1). The predicted molecular masses and isoelectric points for the majority of the identified proteins were consistent with the

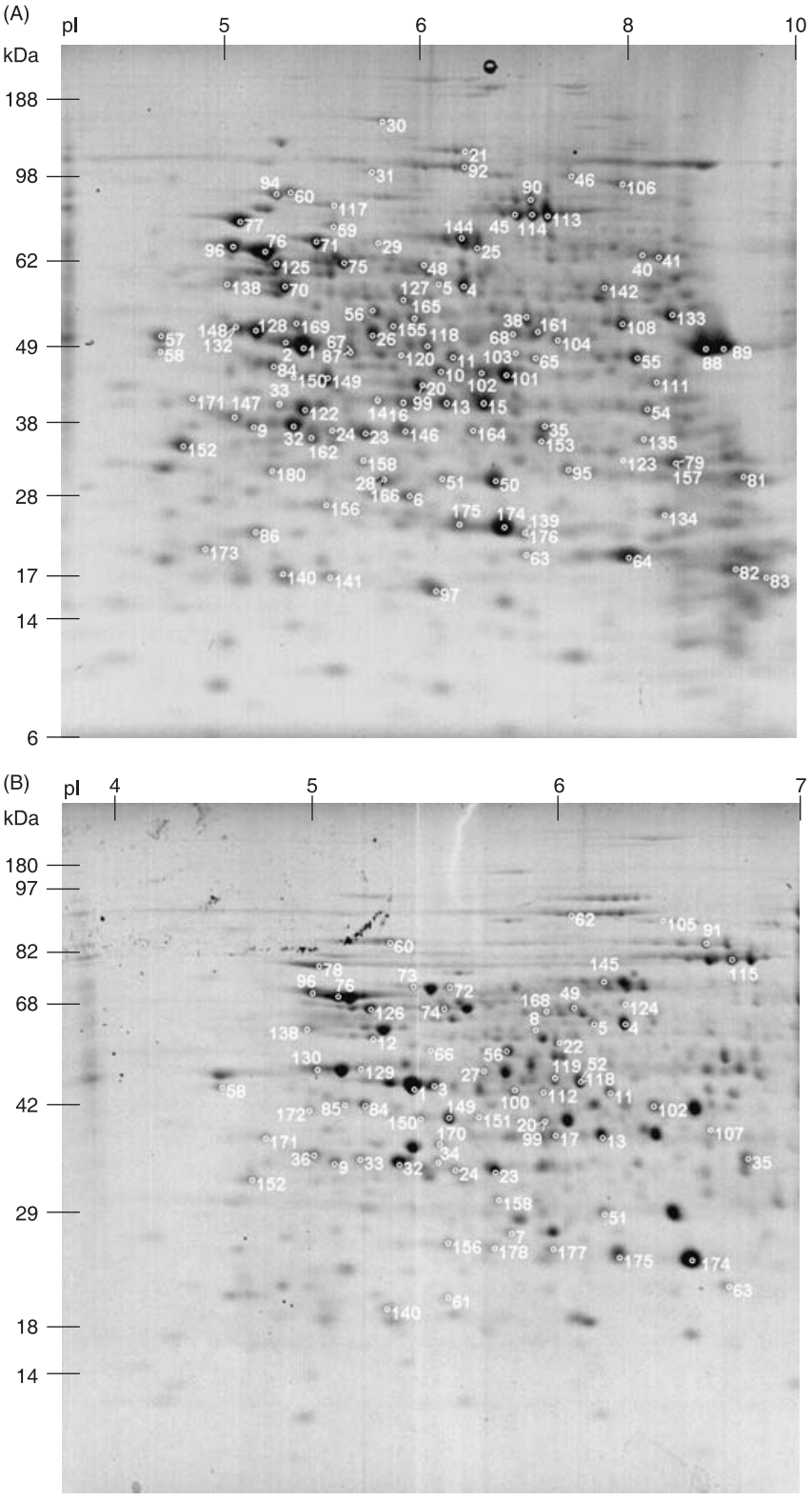

Fig. 2 Coomassie blue-stained two-dimensional gels of *Blumeria graminis* f.sp. *hordei* (*Bgh*) protein extracts. The photographs show two-dimensional gel electrophoresis gels of 160 μg total *Bgh* protein separated on a pI 3–10 (A), pI 4–7 (B) or pI 6–10 (C) gel. Please note that the following spots co-migrate: 20 and 99, 28 and 166, 67 and 87, 79 and 157, 132 and 148, 139 and 176 (A); 20 and 99, 52 and 118 (B); 18 and 54, 19 and 159, and 35, 153 and 163 (C).

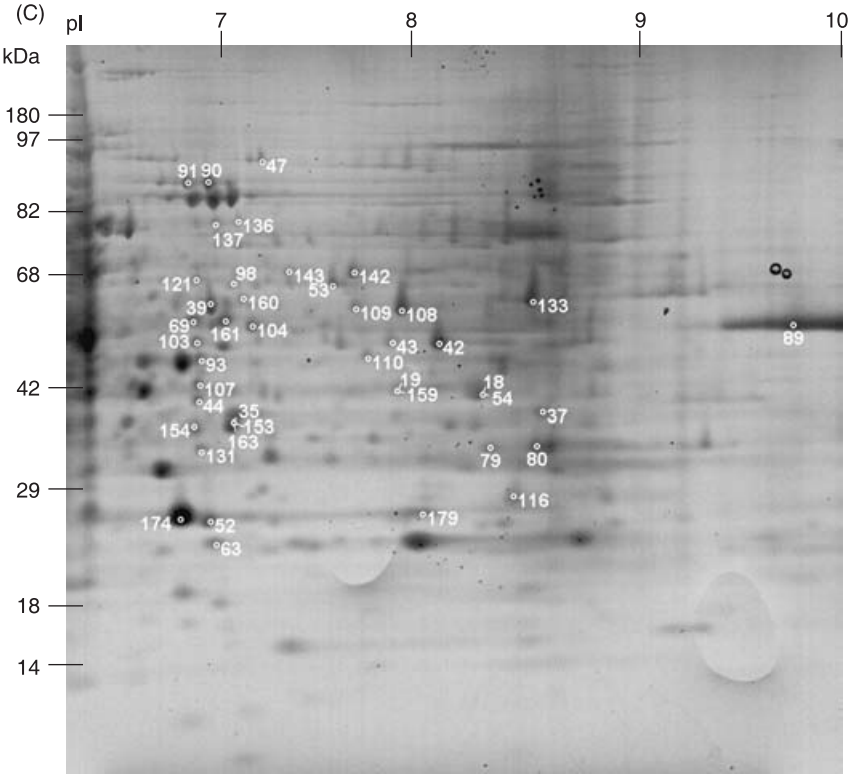

Fig. 2 *Continued.*

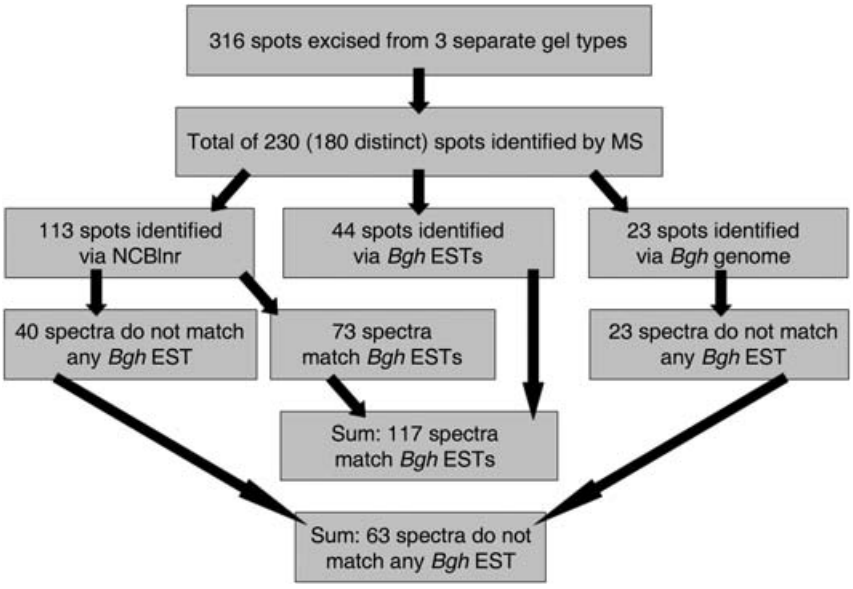

Fig. 3 Flow chart of protein identification. The diagram illustrates the course of the protein identification process. EST, expressed sequence tag; MS, mass spectrometry; NCBInr, National Center for Biotechnology Information non-redundant database.

experimental data, as judged from the location of the respective polypeptide spots within the two-dimensional gels. This further corroborates the predicted identity of the recognized polypeptides. Exceptions include, for example, spots 42, 52 and 147, which exhibited a higher molecular mass than calculated. Conversely, products related to spots such as 62, 125 and 138 showed a lower molecular mass compared with the calculated value. Likewise, the location of some spots within the gels did not conform to the calculated pI (see Table 1 for details). These deviations could result from atypical migration in the

Fig. 4 Venn diagram showing the distribution of protein spots in the various gel types. The diagram illustrates the dispersal and overlap of the identified polypeptide spots in the various two-dimensional gel electrophoresis gels having separate pI ranges.

two-dimensional gels, from post-translational modifications or from partial degradation of intact proteins during the extraction procedure. Given the indirect identification of most polypeptides via fungal species other than *Bgh*, interspecies variation could also explain these discrepancies. After functional classification of the identified proteins (see below), all analysed proteins were designated with unique spot numbers indicated on the corresponding gels shown in Fig. 2. Taken together, this analysis provides a first reference map of the *Bgh* spore proteome.

Presence of polypeptide isoforms

Identical functional annotations of distinct spots may result from either post-translational modifications of the same gene product or from the presence of sequence-related isoforms (paralogues) encoded by distinct genes. In the case of species for which no fully annotated genome sequence is available, these two scenarios are often difficult or even impossible to distinguish on the basis of MS data. Owing to this constraint, we cannot provide an exact number of distinct gene products identified in our study, but base our estimate on two simplifying assumptions. Firstly, two distinct spots whose best matches from the NCBInr database come from different species may represent paralogues rather than modified forms of the same protein, as the respective data sets appear to 'select' distinct sequences. However, as the different hits may also arise from variations in spectral quality, and because we have not performed exhaustive spectral and sequence comparisons to determine uniqueness, even true paralogues may remain unresolved in our survey. Alternatively, modified forms of the same protein could also selectively match different sequences. Secondly, horizontal strings of spots in conjunction with identical identification almost certainly indicate a single gene product with post-translational modifications that change the pI, but not the observed molecular mass (e.g. phosphorylation). In our analysis, examples of this type comprise spots 13–17, 32–36 and 38–39. Based on these simplifying criteria, we estimate that the 180 distinct spots identified in our study represent at least 123 unique proteins.

Functional classification

Predicted functional categories were allocated to the identified proteins based on the biological process annotation routine of PANTHER software (Mi *et al.*, 2007; Thomas *et al.*, 2003; http://www.pantherdb.org/). This assignment was completed manually when proteins well described in the literature were not allotted any function. In total, proteins corresponding to 161 spots were assigned to a PANTHER biological process heading. Six annotated polypeptides were not linked to a biological process heading, and 13 spots (six of which have the same identification) correspond to hypothetical proteins without functional annotation. This indicates that a few of the proteins are novel or uncharacterized polypeptides involved in unidentified cellular processes, some of which may be specific to the biotrophic lifestyle and/or pathogenicity.

Most of the proteins identified are classified as metabolic proteins (almost 75%; Fig. 5). Metabolic polypeptides are often highly abundant soluble proteins and are thus generally well represented in proteomic studies. This also applies to the analysis of fungal proteomes, where metabolic proteins accounted, for example, for 66% of the proteins identified in the uredospores of the phytopathogenic basidiomycete *U. appendiculatus* (Cooper *et al.*, 2006). Likewise, 65% of the polypeptides identified in hyphal forms of the ascomycete *Candida albicans*, a major systemic pathogen of humans, correspond to metabolic proteins (Hernández *et al.*, 2004), although only 20% of the ORFs in *C. albicans* encode proteins devoted to metabolism (Yin *et al.*, 2004). Taken together, it appears that dormant asexual fungal spores exhibit an abundance of metabolic proteins similar to metabolically active fungal hyphae. This suggests that, in spores, the molecular machinery required for energy production and the biogenesis of cellular compounds that are necessary for and after spore germination is preformed to rapidly initiate vegetative growth.

In detail, 27% of the identified polypeptides are involved in carbohydrate metabolism (Fig. 5). Several of these proteins are responsible for energy production, such as citrate synthase and lyase, α-ketoglutarate dehydrogenase and malate dehydrogenase, which are all involved in the tricarboxylic acid cycle. Others, for example enolase, pyruvate kinase, pyruvate dehydrogenase, phosphoglycerate kinase, phosphoglyceromutase, phosphoglucomutase, glyceraldehyde-3-phosphate dehydrogenase and fructose-bisphosphate aldolase, are important enzymes of glycolysis

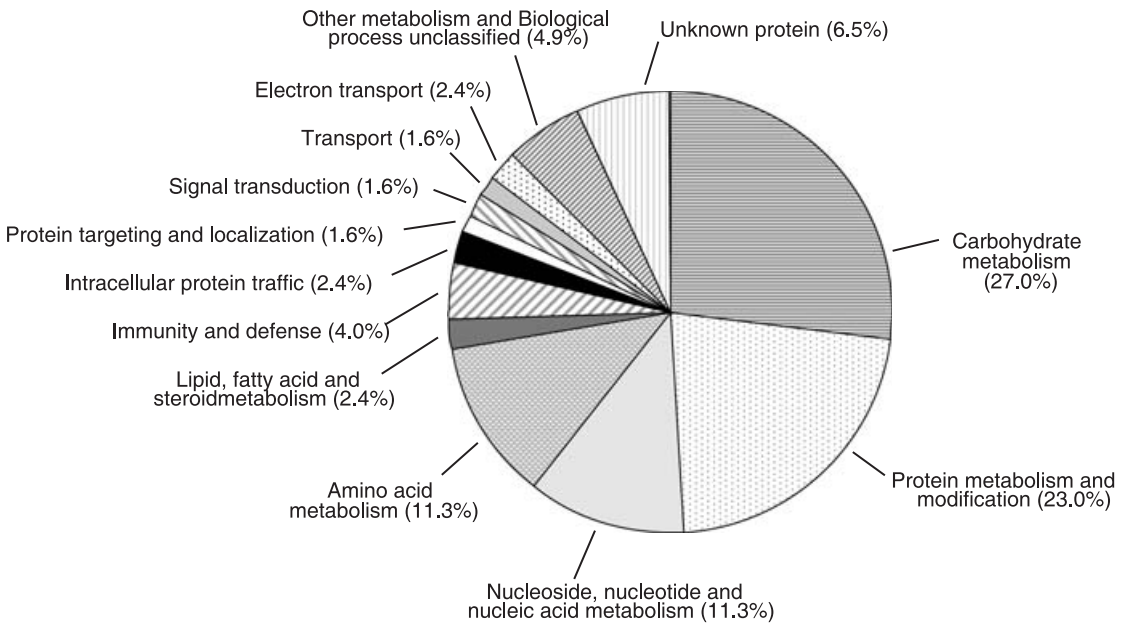

Fig. 5 Pie chart representing the functional classification of the identified proteins. The diagram shows the relative abundance of the identified proteins in the various functional categories of the PANTHER classification system. To avoid a potential imbalance owing to polypeptides that may be represented by multiple spots, the calculation is based on the set of 123 spots that probably represent distinct polypeptides.

and/or gluconeogenesis. Additional identified enzymes (e.g. transaldolase, transketolase and 6-phosphogluconate dehydrogenase) catalyse reactions of the pentose phosphate pathway, and the glycogen branching enzyme is part of glycogen metabolism. Polypeptides involved in lipid, fatty acid and steroid metabolism represent approximately 2% of the classified proteins (Fig. 5). Glycogen and lipids have been described as major storage forms of carbon and energy in *Bgh* conidia, and it has been suggested that glycogen and lipid catabolism represent key sources of energy allocation in germinating powdery mildew conidia (Both *et al.*, 2005a). Our proteomic analysis supports this assumption, indicating that crucial enzymes of these catabolic pathways are preformed in conidia, enabling swift energy conversion during spore germination.

Another functional category represented by multiple members is devoted to protein metabolism and modification (23% of the identified polypeptides; Fig. 5). This class includes various proteins with distinct functions, such as different peptidases, cyclophilins (peptidyl-prolyl *cis*/*trans*-isomerases), heat shock proteins, ribosomal proteins and translation/elongation factors. Taken together, these polypeptides point to a key role for protein biosynthesis and folding in *Bgh* conidia. This scenario is reminiscent of the situation in uredospores of the biotrophic bean rust fungus *U. appendiculatus*, where the majority of the identified polypeptides were also found to be involved in protein assembly and catabolism (Cooper *et al.*, 2006). It seems that both *Bgh* conidiospores and rust uredospores are pre-equipped with the necessary components to initiate protein production rapidly on germination.

Components of amino acid metabolism make up approximately 11% of the identified proteins (Fig. 5). In a broader sense, proteins of this class also contribute to protein biosynthesis and turnover, thus further corroborating the above-mentioned hypothesis. Biological processes related to nucleoside, nucleotide and nucleic acid metabolism also account for roughly 11% of the polypeptides identified in our analysis (Fig. 5). In addition, a number of annotated proteins (4%; Fig. 5) are well-known stress response or cell defence proteins. They are mainly redox regulatory proteins (e.g. peroxiredoxin, catalase, peroxidase) involved in protection against oxidative stress. Pathogenic microbes often trigger a localized oxidative burst in their host species at sites of attempted invasion (Hückelhoven and Kogel, 2003). The identified antioxidative proteins may be required for protection against this presumptive plant defence response (Zhang *et al.*, 2004). The remaining identified proteins were associated with intracellular protein traffic, protein targeting and localization, signal transduction, transport and electron transport (around 2% each; Fig. 5).

CONCLUSIONS

Our study has generated the first annotated proteome map of a powdery mildew fungus. It corroborates the hypothesis that asexual fungal spores, like pollen grains of plants (Holmes-Davis

Table 1 *Blumeria graminis* f.sp. *hordei* (*Bgh*) proteins identified in this study†.

Spot name‡	2D gel§	Accession/EST/ genomic *Bgh* sequence	Match with *Bgh* EST¶	Description††	Species††	pI/obs.‡‡	MM (kDa)/obs‡‡	Cov. [%]§§	Mascot score§§
Carbohydrate metabolism									
1	A,B	**GI:74612186**	✓	Enolase	*Tuber borchii*	5.3	47.9	8	**342**
2	A	**GI:74612186**	✓	Enolase	*Tuber borchii*	5.3	47.9	13	**376**
3	B	**GI:74612186**	✓	Enolase	*Tuber borchii*	5.3	47.9	8	**332**
4	A,B	**GI:115390717**	✓	Pyruvate kinase	*Aspergillus terreus*	6.7	58.1	2.3	**112**
5	A,B	**GI:115390717**	✓	Pyruvate kinase	*Aspergillus terreus*	6.7	58.1	2.3	**55**
6	A	**AW789899**		Triosephosphate isomerase (GI:156040910)	*Sclerotinia sclerotiorum*	5.5	27	n.a.	**164***
7	B	**AW789899**		Triosephosphate isomerase (GI:156040910)	*Sclerotinia sclerotiorum*	5.5	27	n.a.	**152***
8	B	**GI:52352519**	✓	Phosphoglucomutase (PGM1)	*Saccharomyces kudriavzevii*	5.3	60.6	3.5	**76**
9	A,B	**GI:70986482**	✓	Pyruvate dehydrogenase E1 β subunit, hyp. prot.	*Aspergillus fumigatus*	7.6/5	40.5/35	6.6	**151**
10	A	**GI:115390821**		Pyruvate dehydrogenase E1 α subunit	*Aspergillus terreus*	8.5/6	45.3	4.4	**81**
11	A,B	**GI:110763826**	✓	Phosphoglycerate kinase, hyp. prot.	*Apis mellifera*	9	45	3.4	**65**
12	B	**BQ284104**		Phosphoglyceromutase, hyp. prot. (GI:156042436)	*Sclerotinia sclerotiorum*	5.1	57.2	n.a.	**180**
13	A,B	**GI:2494638**	✓	Glyceraldehyde-3-phosphate dehydrogenase (GAPDH)	*Blumeria graminis*	6	36.5	79	**633**
14	A	**GI:2494638**		Glyceraldehyde-3-phosphate dehydrogenase (GAPDH)	*Blumeria graminis*	6/5.7	36.5/40	7.1	**170**
15	A	**GI:2494638**	✓	Glyceraldehyde-3-phosphate dehydrogenase (GAPDH)	*Blumeria graminis*	6/6.5	36.5/40	76.9	**680**
16	A	**GI:2494638**	✓	Glyceraldehyde-3-phosphate dehydrogenase (GAPDH)	*Blumeria graminis*	6	36.5/40	58	**173**
17	B	**GI:2494638**	✓	Glyceraldehyde-3-phosphate dehydrogenase (GAPDH)	*Blumeria graminis*	6	36.5/40	67.2	**342**
18	C	**GI:2494638**		Glyceraldehyde-3-phosphate dehydrogenase (GAPDH)	*Blumeria graminis*	6/8	36.5/40	7.1	**129**
19	C	**GI:2494638**		Glyceraldehyde-3-phosphate dehydrogenase (GAPDH)	*Blumeria graminis*	6/7.5	36.5/40	10.7	**181**
20	A,B	**AW790282**		Fructose-bisphosphate aldolase (GI:154314989)	*Botryotinia fuckeliana*	5.4	39	n.a.	**327**
21	A	**GI:156036300**		Pyruvate carboxylase, hyp. prot.	*Sclerotinia sclerotiorum*	6.1	132.5	14.6	**86***
22	B	**Contig_9627**		Glucose-6-phosphate isomerase, putative (GI:111057935)	*Phaeosphaeria nodorum*	5.9	61	22.2	**89***
23	A,B	**GI:68481811**	✓	Transaldolase	*Candida albicans*	4.8	35.7	6.5	**102**
24	A,B	**GI:68481811**	✓	Transaldolase	*Candida albicans*	4.8	35.7	3.7	**63**
25	A	**GI:50423907**		Transketolase, hyp. prot.	*Debaryomyces hansenii*	6.1	75.4	3	**117**
26	A	**GI:119469246**	✓	6-Phosphogluconate dehydrogenase, decarboxylating	*Neosartorya fischeri*	5.9	55.8	7.3	**145**
27	B	**GI:85115938**	✓	6-Phosphogluconate dehydrogenase, hyp. prot.	*Neurospora crassa*	6.3/5.7	57.2	2.3	**75**
28	A	**Contig_5253**		6-Phosphogluconolactonase, hyp. prot. (GI:156051562)	*Sclerotinia sclerotiorum*	5.5	28.9	50.4	**143**
29	A	**GI:118083730**	✓	Glycogen branching enzyme, hyp. prot.	*Gallus gallus*	6	80.1	1.7	**78**
30	A	**Contig_2726**		Glycosidase, putative (GI:154314369)	*Botryotinia fuckeliana*	5.8	174	32.4	**247***
31	A	**GI:39947727**	✓	Glycosyl hydrolase, hyp. prot.	*Magnaporthe grisea*	5.8	110.6	1.2	**61**
32	A,B	**GI:67537722**	✓	Malate dehydrogenase, hyp. prot.	*Aspergillus nidulans*	5.7	33.6	3.4	**96**
33	A,B	**GI:67537722**	✓	Malate dehydrogenase, hyp. prot.	*Aspergillus nidulans*	5.7	33.6	3.4	**84**
34	B	**AW788156**		Malate dehydrogenase, hyp. prot. (GI:156048488)	*Sclerotinia sclerotiorum*	6.7/5.5	34.5	n.a.	**87**
35	A,B,C	**GI:5123836**	✓	Malate dehydrogenase	*Nicotiana tabacum*	9/7	43.3	5.6	**114**
36	B	**AW788156**		Malate dehydrogenase, hyp. prot. (GI:156048488)	*Sclerotinia sclerotiorum*	6.7/5	34.5	n.a.	**73**
37	C	**GI:5929964**	✓	Malate dehydrogenase	*Glycine max*	9.1	36.1	3.5	**121**
38	A	**GI:7160184**	✓	ATP citrate lyase, subunit 2	*Sordaria macrospora*	5.5/7	52.2	3.5	**134**
39	C	**GI:70992211**	✓	ATP citrate lyase subunit, hyp. prot.	*Aspergillus nidulans*	5.8/7	53	31	**216**
40	A	**GI:119471597**	✓	ATP citrate lyase, subunit 1, hyp. prot.	*Neosartorya fischeri*	9.3	71.9/62	6.4	**316**
41	A	**GI:121699808**	✓	ATP citrate synthase subunit 1	*Magnaporthe grisea*	9.2	72.4/62	26	**100***
42	C	**GI:116500157**	✓	Citrate synthase type I, hyp. prot.	*Coprinopsis cinerea*	9.5/8	16.8/45	9.3	**103**
43	C	**Contig_11872_107 + 11872_116**		Citrate synthase (GI:156063018)	*Sclerotinia sclerotiorum*	7.2	50	13.8	**91**
44	C	**Contig_7973**		Isocitrate dehydrogenase, hyp. prot. (GI:119183931)	*Coccidioides immitis*	8.9/7	41	41.8	**179**
45	A	**GI:27803048**	✓	Aconitate hydratase, hyp. prot.	*Podospora anserina*	6.4	85.1	1.7	**71**
46	A	**Contig_3948**		α-Ketoglutarate decarboxylase (GI:156054172)	*Sclerotinia sclerotiorum*	6.3/8	118	17.2	**106***
47	C	**GI:67538802**		α-Ketoglutarate dehydrogenase, subunit, hyp. prot.	*Aspergillus nidulans*	6.4/7	117/97	9.3	**75**
48	A	**GI:67524917**	✓	Succinate dehydrogenase flavoprotein subunit, hyp. prot.	*Aspergillus nidulans*	6.1	69.4	22.3	**74***
49	B	**GI:71000275**		Succinate dehydrogenase subunit, hyp. prot.	*Aspergillus fumigatus*	6.5	71.1	2.3	**72**
50	A	**GI:14550183**	✓	NADP-dependent mannitol dehydrogenase	*Cladosporium fulvum*	6.1	28.6	4.1	**54**
51	B,A	**GI:14550183**	✓	NADP-dependent mannitol dehydrogenase	*Cladosporium fulvum*	6.1	28.6	4.1	**50**
52	C,B	**GI:14550183**	✓	NADP-dependent mannitol dehydrogenase	*Cladosporium fulvum*	6.1	28.6/50	4.1	47
53	C	**GI:46107282**	✓	UDP-glucose pyrophosphorylase, hyp. prot.	*Gibberella zeae*	6.1	57.1	7.8	**267**
54	A,C	**AW788419**		Nucleoside-diphosphate-sugar epimerase, hyp. prot. (GI:111063143)	*Phaeosphaeria nodorum*	6.3/8	38/40	n.a.	**220**
55	A	**GI:111070271**		Serine hydroxymethyltransferase, hyp. prot.	*Phaeosphaeria nodorum*	9.2	51.6	6.9	**170**
56	A,B	**Contig_14052**		Dehydrogenase acyltransferase (GI:156031305)	*Sclerotinia sclerotiorum*	5.5	48	59.8	**156***
Protein metabolism and modification									
57	A	**AW792643**		Serine carboypeptidase, hyp. prot. (GI:85081820)	*Neurospora crassa*	5.2/4.8	62/50	n.a.	**448**
58	A,B	**AW792643**		Serine carboypeptidase, hyp. prot. (GI:85081820)	*Neurospora crassa*	5.2/4.8	62/49	n.a.	**402**
59	A	**GI:119178714**	✓	Zn-dependent oligopeptidase, hyp. prot.	*Coccidioides immitis*	5.7	82.1	1.4	**75**

Table 1 *Continued.*

Spot name‡	2D gel§	Accession/EST/ genomic *Bgh* sequence	Match with *Bgh* EST¶	Description††	Species††	pI/obs.‡‡	MM (kDa)/obs‡‡	Cov. [%]§§	Mascot score§§
60	A,B	**BM361215**		Aminopeptidase (GI:121707310)	*Aspergillus clavatus*	5.1	98.4	n.a.	**119**
61	B	**AW787940**		Aminopeptidase, hyp. prot. (GI:154296638)	*Botryotinia fuckeliana*	5.9	56.4/25	n.a.	**39**
62	B	**GI:146452516**		Secreted/periplasmic Zn-dependent peptidase, hyp. prot.	*Lodderomyces elongisporus*	6.6	130.6/95	1.2	**27 (84)**
63	A,B,C	**BQ284067**		Cyclophilin, hyp. prot. (GI:154313502)	*Botryotinia fuckeliana*	5.2	31.6	n.a.	**312**
64	A	**AW788820**		Cyclophilin 1, hyp. prot. (GI:33357681)	*Botryotinia fuckeliana*	9.1	24.2	n.a.	**194***
65	A	**GI:27805447**	✓	Cyclophilin	*Paramecium primaurelia*	9.6/7	17.7/45	7.4	**68**
66	B	**GI46110292**	✓	ATP-dependent 26S proteasome regulatory subunit, hyp. prot.	*Gibberella zeae*	5	28.6/60	6.5	**100**
67	A	**GI:46138509**		26S protease regulatory subunit 6B, hyp. prot.	*Gibberella zeae*	5.3	46.9	52	**135***
68	A	**GI:119496777**		DNAJ-class molecular chaperone, hyp. prot.	*Neosartorya fischeri*	5.7	45.4	3.6	**73**
69	C	**GI:119189679**		DNAJ-class molecular chaperone, hyp. prot.	*Coccidioides immitis*	6	45.3	3.6	44
70	A	**GI:119182507**	✓	Heat shock protein 60	*Coccidioides immitis*	5.4	62.4	33.8	**92***
71	A	**GI:39944360**		Heat shock protein 70, hyp. prot.	*Magnaporthe grisea*	5.8	72.6	3.7	**207**
72	B	**GI:121715382**		Heat shock protein 70	*Aspergillus clavatus*	5.7	72.5	2.3	**36 (215)**
73	B	**GI:39944360**		Heat shock protein 70, hyp. prot.	*Magnaporthe grisea*	5.8	72.6	15.8	**38 (199)**
74	B	**GI:116182094**		Heat shock protein 70	*Chaetomium globosum*	5.1	67	5.6	**278**
75	A	**GI:70983346**		Heat shock protein 70, hyp. prot.	*Aspergillus fumigatus*	5.2	66.9	21	**312**
76	A,B	**GI:42477037**	✓	Heat shock protein 70	*Trichophyton verrucosum*	4.9	70.8	38.1	**147***
77	A	**GI:123666**	✓	Heat shock protein 83	*Trypanosoma brucei brucei*	5	80.7	5.3	**233**
78	B	**GI:9837418**	✓	Heat shock protein 90	*Tetrahymena pyriformis*	5	80.8	3.4	**111**
79	A,C	**GI:85078476**	✓	40S ribosomal protein S3	*Neurospora crassa*	9.6	28.8	43.7	**178***
80	C	**GI:85078476**		40S ribosomal protein S3	*Neurospora crassa*	9.6	28.8	36.9	**79***
81	A	**GI:115402405**	✓	40S ribosomal protein S2	*Aspergillus terreus*	11.1	28.2	5.4	**62**
82	A	**GI:46123785**	✓	40S ribosomal protein S10, hyp. prot.	*Gibberella zeae*	10.2	19.1	11.2	**278**
83	A	**GI:46138661**	✓	50S ribosomal protein, hyp. prot.	*Gibberella zeae*	11.3/9.8	15.4	6.6	**55**
84	A,B	**GI:119177270**	✓	Eukaryotic translation/initiation factor 4	*Coccidioides immitis*	4.9/5.4	44.8	38	**304**
85	B	**GI:71000162**		Eukaryotic translation initiation factor 4, hyp. prot.	*Aspergillus fumigatus*	4.9	45.7	7.4	**127**
86	A	**GI:729823**	✓	Eukaryotic translation initiation factor 5A	*Neurospora crassa*	5.4	18.1	7.4	**105**
87	A	**AW790050**	✓	Elongation factor 1γ (GI:85101774)	*Neurospora crassa*	5.5	45.4	n.a.	**273**
88	A	**GI:17027007**	✓	Elongation factor-1α	*Pycnocentrodes sp.*	9.5	39.4	3	**63**
89	A,C	**GI:17027007**	✓	Elongation factor-1α	*Pycnocentrodes sp.*	9.5	39.4	6.1	**91**
90	A,C	**GI:85106981**		Elongation factor 2	*Neurospora crassa*	6.3	93.2	26.1	**145**
91	B,C	**GI:85106981**		Elongation factor 2	*Neurospora crassa*	6.3	93.2/82	14.2	**104**
92	A	**GI:83765350**	✓	Elongation factor 3, conserved domains	*Aspergillus oryzae*	5.9	117.8	4.8	**214**
93	C	**AW791437**		Acetyl-CoA acetyltransferase, hyp. prot. (GI:156040271)	*Sclerotinia sclerotiorum*	6.6	41.8	n.a.	**92**
94	A	**GI:39940094**	✓	Cell division control protein (Cdc48)	*Magnaporthe grisea*	4.8	89.9	39.9	**194**
95	A	**AW790865**		Serine protease 2 (GI:17385556)	*Pyrenopeziza brassicae*	5.8	55.6	n.a.	**301**
96	A,B	**GI:85080590**	✓	Glucose-regulated protein homologue precursor (GRP 78)	*Neurospora crassa*	4.9	72.3	3.2	**104**
97	A	**BM361602**		Actin depolymerization factor/cofilin-like, hyp. prot. (GI:46123735)	*Gibberella zeae*	5.2/6	16.1	n.a.	**94**
98	C	**contig_10677**		UDP-*N*-acetylglucosamine pyrophosphorylase (GI:156053648)	*Sclerotinia sclerotiorum*	5.4/7	56	24.6	**70***
Amino acid metabolism									
99	A,B	**AW789533**		Glutamine synthetase (GI:154298092)	*Sclerotinia sclerotiorum*	5.5	40.1	n.a.	**103**
100	B	**Contig_1225**		Argininosuccinate synthetase (GI:156057843)	*Sclerotinia sclerotiorum*	5.1	45	38.2	**168***
101	A	**GI:70995343**	✓	*S*-Adenosylmethionine synthetase	*Aspergillus fumigatus*	5.6	42.2	21	**211**
102	A,B	**GI:119495861**	✓	*S*-Adenosylmethionine synthetase	*Neosartorya fischeri*	5.5	42.1	26	**170**
103	A,C	**GI:116205243**		Chorismate synthase, hyp. prot.	*Chaetomium globosum*	6.5	45.6	21	45, 77*
104	A,C	**GI:39946672**	✓	Saccharopine dehydrogenase	*Magnaporthe grisea*	6.1/7	49.1	3.8	**73**
105	B	**Contig_7205**		Glycine dehydrogenase, hyp. prot. (GI:156058930)	*Sclerotinia sclerotiorum*	6	116/95	18.3	**90***
106	A	**Contig_11926**		Putative dehydrogenase/cyclohydrolase (GI:156059764)	*Sclerotinia sclerotiorum*	6.3/8	101	18.1	**150***
107	B,C	**Contig_5443**		Cystathionine gamma-lyase, hyp. prot. (GI:156063172)	*Sclerotinia sclerotiorum*	6.2	45	37.2	**164***
108	A,C	**GI:70999940**	✓	Serine hydroxymethyltransferase, hyp. prot.	*Aspergillus fumigatus*	8.6	51.8	7.6	**198**
109	C	**GI:85094603**	✓	Serine hydroxymethyltransferase	*Neurospora crassa*	7.1	52.9	3.3	**132**
110	C	**AW790371**		Aminomethyltransferase, hyp. prot. (GI:156053183)	*Sclerotinia sclerotiorum*	9.1/7.5	50.7	n.a.	**113***
111	A	**GI:46138463**		Aspartate/tyrosine/aromatic aminotransferase, hyp. prot.	*Gibberella zeae*	9.3	46.6	3.8	**57**
112	B	**contig_5844**		Aspartate/tyrosine/aromatic aminotransferase, hyp. prot. (GI:156030852)	*Sclerotinia sclerotiorum*	5.4	46	37.8	**123**
113	A	**GI:47132400**	✓	Methionine synthase	*Pichia pastoris*	5.8/6.5	85.9	1.3	**81**
114	A	**GI:6969602**	✓	Methionine synthase	*Cladosporium fulvum*	6.4	87.1	2.7	**156**
115	B	**GI:68475194**	✓	Putative cobalamin-independent methionine synthase	*Candida albicans*	5.3/6.5	85.6	1.3	**70**

Table 1 *Continued.*

Spot name‡	2D gel§	Accession/EST/ genomic *Bgh* sequence	Match with *Bgh* EST¶	Description††	Species††	pI/obs.‡‡	MM (kDa)/obs‡‡	Cov. [%]§§	Mascot score§§
Nucleoside, nucleotide and nucleic acid metabolism									
116	C	**GI:67538624**	✓	GTP-binding nuclear protein (RAN/TC4)	*Aspergillus nidulans*	7.7/8.5	24.9/30	6.3	**73**
117	A	**AW789762**		Polyadenylate-binding protein (GI:115390925)	*Aspergillus terreus*	5.7	81.8	n.a.	**63**
118	A,B	**GI:85107784**	✓	Adenosylhomocysteinase, hyp. prot.	*Neurospora crassa*	5.8	49	28.5	**116***
119	B	**BM361451**		Adenosylhomocysteinase (GI:156062152)	*Sclerotinia sclerotiorum*	5.6	48.9	n.a.	**79***
120	A	**BM361451**		Adenosylhomocysteinase (GI:156062152)	*Sclerotinia sclerotiorum*	5.6	48.9	n.a.	**68***
121	C	**GI:115442686**	✓	Inosine-5′-monophosphate dehydrogenase	*Aspergillus terreus*	6.6	58.1	2.7	**68**
122	A	**Contig_6578**		Adenosine kinase (GI:154311437)	*Botryotinia fuckeliana*	5.4	37	50.4	**163***
123	A	**Contig_4185**		Adenylate kinase (GI:156062980)	*Sclerotinia sclerotiorum*	8.6	28	36.9	**90***
124	B	**Contig_10205**		Purine biosynthesis protein, hyp. prot. (GI:85111684)	*Sclerotinia sclerotiorum*	6	65	40.2	**79***
125	A	**GI:46125253**		Vacuolar ATPase subunit A, hyp. prot.	*Gibberella zeae*	6.7/5.3	91.9/62	30.8	**96***
126	B	**GI:111060400**		Vacuolar ATPase subunit A, hyp. prot.	*Phaeosphaeria nodorum*	6.6/5.3	43.8/65	24.2	**78***
127	A	**GI:46107508**		Vacuolar ATPase subunit B	*Gibberella zeae*	5.3	56.6	31.5	**117***
128	A	**GI:111606563**		ATP synthase β chain	*Coccidioides posadasii*	5.1	55.9	46.8	**115***
129	B	**GI:119182499**		ATP synthase β chain	*Coccidioides immitis*	5.1	55.8	16.1	**85***
130	B	**GI:46116940**		ATP synthase β chain	*Gibberella zeae*	5.3	54.9	19.7	66*
131	C	**AW787925**		ATP synthase γ chain, hyp. prot. (GI:156045651)	*Sclerotinia sclerotiorum*	8.3/6.5	32.1	n.a.	**61***
132	A	**GI:171110**		F1-ATPase β subunit	*Saccharomyces cerevisiae*	5.6	54.9	5.7	**147**
133	A,C	**GI:39972915**		F1-ATPase α-subunit	*Magnaporthe grisea*	9.8/8.5	59.5	39	**244**
134	A	**GI:70990878**	✓	ADP, ATP carrier protein, hyp. prot.	*Aspergillus fumigatus*	10.3/8.3	33.3/25	5.2	**177**
Lipid, fatty acid and steroid metabolism									
135	A	**Contig_591_57 + _591_52**		NADH-cytochrome *b*5 reductase (GI:154297211)	*Botryotinia fuckeliana*	9.1	38	49	**178**
136	C	**Contig_4916**		Acyl-CoA synthetase (GI:154290515)	*Botryotinia fuckeliana*	6.9	77	24.4	**86**
137	C	**Contig_4916**		Acyl-CoA synthetase (GI:154290515)	*Botryotinia fuckeliana*	6.9	77	9	**72**
138	A,B	**BM361770**		Esterase lipase, hyp. prot. (GI:85093411)	*Neurospora crassa*	7.5/5	121.6/60	n.a.	**129**
Immunity and defence									
139	A	**GI:18033107**	✓	Superoxide dismutase	*Blumeria graminis*	6.4	24.2	56	**354**
140	A,B	**BM360950**		Peroxiredoxin, hyp. prot. (GI:154312864)	*Botryotinia fuckeliana*	5.3	16	n.a.	**151**
141	A	**BM360950**		Peroxiredoxin, hyp. prot. (GI:154312864)	*Botryotinia fuckeliana*	5.7	16.3	n.a.	**43**
142	A,C	**GI:70982394**	✓	Oxidoreductase related to apoptosis-inducing factor like, hyp. prot.	*Aspergillus fumigatus*	8.6	59.8	2.2	**70**
143	C	**AW792600**		Oxidoreductase related to apoptosis-inducing factor like, hyp. prot. (GI:154304889)	*Botryotinia fuckeliana*	6.3	58.1	n.a.	**51**
144	A	**GI:18033118**	✓	Catalase/peroxidase	*Blumeria graminis*	7.3	87.5	59.3	**301***
145	B	**GI:18033118**	✓	Catalase/peroxidase	*Blumeria graminis*	7.3	87.5	24.7	**141***
146	A	**GI:71012754**		Ascorbate peroxidase, hyp. prot.	*Ustilago maydis*	9/6	43.1	4.8	**128**
Intracellular protein traffic									
147	A	**GI:111060927**	✓	Hyp. prot. with RAN binding site	*Phaeosphaeria nodorum*	4.8	28.1 /40	13.7	**214**
148	A	**GI:135481**		Tubulin β chain	*Blumeria graminis*	4.7	49.7	46.2	**134***
149	A,B	**GI:67540744**		Actin	*Aspergillus nidulans*	5.5	41.7	66.2	**261***
150	A,B	**GI:67540744**		Actin	*Aspergillus nidulans*	5.5	41.7	67.8	**268***
151	B	**GI:67540744**		Actin	*Aspergillus nidulans*	5.5	41.7	32.7	**115***
Protein targeting and localization									
152	A,B	**GI:85113087**	✓	14-3-3 protein homologue	*Neurospora crassa*	4.6	29.3	33.2	**83***
153	A,C	**GI:3023852**	✓	Guanine nucleotide-binding protein subunit β-like protein	*Neurospora crassa*	7	35.1	5.7	**160**
154	C	**GI:39945474**		Guanine nucleotide-binding protein subunit β-like protein, hyp. prot.	*Magnaporthe grisea*	6.9	35	5.7	**140**
Signal transduction									
155	A	**GI:396431**	✓	Rab guanosine diphosphate dissociation inhibitor α	*Rattus norvegicus*	4.9	50.5	4.3	**143**
156	A,B	**AW791753**		RHO protein GDP dissociation inhibitor, hyp. prot. (GI:156049611)	*Sclerotinia sclerotiorum*	5.1	22.5	n.a.	**79***
Transport									
157	A	**AW789658**		Porin (GI:154316512)	*Botryotinia fuckeliana*	9	29.9	n.a.	**109**
158	A,B	**Contig_8027**		ABC transporter signature motif (GI:154305908)	*Botryotinia fuckeliana*	6.5	31	27.8	**265**
Electron transport									
159	C	**AW790540**		NADH-ubiquinone oxidoreductase 40 kDa subunit (GI:154289498)	*Botryotinia fuckeliana*	9.4/8	28.5/40	n.a.	**106**
160	C	**AW790630**		Glutathione reductase, hyp. prot. (GI:154291666)	*Botryotinia fuckeliana*	6.3	51	n.a.	**90**
161	A,C	**GI:19114408**	✓	Dihydrolipoamide dehydrogenase, hyp. prot.	*Schizosaccharomyces pombe*	9.5/7	54.7	2.2	**92**

Table 1 *Continued.*

Spot name‡	2D gel§	Accession/EST/ genomic *Bgh* sequence	Match with *Bgh* EST¶	Description††	Species††	pI/obs.‡‡	MM (kDa)/obs‡‡	Cov. [%]§§	Mascot score§§
Other metabolism or biological process unclassified									
162	A	**GI:6325326**		Spermidine synthase	*Saccharomyces cerevisiae*	5.2	33.3	4.4	**91**
163	C	**AW790589**		NAD(P)H-dependent D-xylose reductase (GI:67516283)	*Aspergillus terreus*	5.4/7	35.6	n.a.	**78**
164	A	**Contig_6463**		Glycerol dehydrogenase, putative (GI:119480951)	*Neosartorya fischeri*	6.6	35	72.5	**77***
165	A	**BM361761**		Aldehyde dehydrogenase, hyp. prot. (GI:154320197)	*Botryotinia fuckeliana*	5.2	54	n.a.	**128**
166	A	**GI:46116836**		Alcohol dehydrogenase and 3-ketoacyl-acyl-carrier-protein reductase, conserved domains	*Gibberella zeae*	6.4	29	6.3	**86**
167	C	**AW791581**		NAD-binding domain 4 protein (GI:145236573)	*Aspergillus niger*	8.1	48.2	n.a.	**151**
Unknown protein									
168	B	**GI:50294754**		Conserved hyp. prot.	*Candida glabrata*	9.8	96.8	13.4	**76***
169	A	**Contig_3909**		Conserved hyp. prot. (GI:156043053)	*Sclerotinia sclerotiorum*	5.1	53	79.1	**282**
170	B	**Contig_8402_133 + _8402_137**		Conserved hyp. prot. (GI:156058700)	*Sclerotinia sclerotiorum*	6.8/5.5	39	5.2	**52**
171	A,B	**AW790280**		Conserved hyp. prot. (GI:156052649)	*Sclerotinia sclerotiorum*	4.9	36.2/40	n.a.	**135**
172	B	**AW792491**		Conserved hyp. prot. (GI:121712070)	*Aspergillus clavatus*	6.3	41.2	n.a.	**154**
173	A	**AW792723**		Conserved hyp. prot. (GI:156061853)	*Sclerotinia sclerotiorum*	4.8	18	n.a.	**113**
174	A,B,C	**BM361778**		Hyp. prot., no putative conserved domains detected (GI:27453871)	n.a.	n.a.	n.a.	n.a.	**221**
175	A,B	**BM361778**		Hyp. prot., no putative conserved domains detected (GI:27453871)	n.a.	n.a.	n.a.	n.a.	**217**
176	A	**BM361778**		Hyp. prot., no putative conserved domains detected (GI:27453871)	n.a.	n.a.	n.a.	n.a.	**174**
177	B	**BM361778**		Hyp. prot., no putative conserved domains detected (GI:27453871)	n.a.	n.a.	n.a.	n.a.	**172**
178	B	**BM361778**		Hyp. prot., no putative conserved domains detected (GI:27453871)	n.a.	n.a.	n.a.	n.a.	**101**
179	C	**BM361778**		Hyp. prot., no putative conserved domains detected (GI:27453871)	n.a.	n.a.	n.a.	n.a.	**217**
180	A	**BM361783**		Hyp. prot., no putative conserved domains detected (GI:156044082)	*Sclerotinia sclerotiorum*	7	80.9	n.a.	**63**

†For an extended version of this table, see Table S1 and caption.

‡Please note that spots 20 and 101, 28 and 170, 69 and 89, 136 and 152, 143 and 181 (pI 3–10 gel), 20 and 101, 53 and 121 (pI 4–7 gel), as well as 36, 157 and 167 (pI 6–10 gel), co-migrated in the mentioned gel types.

§Gel A, pI 3–10 (Fig. 2A); gel B, pI 4–7 (Fig. 2B); gel C, pI 6–10 (Fig. 2C).

¶A tick indicates that the reported identification/annotation is supported by a significant hit to a homologous *Bgh* expressed sequence tag (EST) in a mass spectrometry (MS) or MS/MS search.

††Description and species origin of the corresponding protein accession or the closest homologue of *Bgh* EST/genomic sequences as determined by BLAST search (see http://blast.ncbi.nlm.nih.gov/Blast.cgi). In the latter cases, GI numbers of BLAST hits are given in parentheses (hyp. prot., hypothetical protein). n.a., not applicable, as no sequence with significant homology in any other species.

‡‡Molecular mass (kDa) and isoelectric point (pI) of the identified protein. These values are given according to ProteinScape software (Bruker Daltonics) when spots were identified by a protein accession. When identified from EST or genomic *Bgh* sequences, the expected pI and molecular masses were determined using the Expasy Compute pI/Mw tool and the best BLAST hit to the partial sequence. When the observed (obs.) molecular mass and/or pI was different from the expected value, both are indicated. n.a., not applicable, as best match is against an EST for which no molecular mass or pI can be calculated.

§§Sequence coverage (percentage of the complete protein sequence; n.a., not applicable, as best match is against an EST for which no sequence coverage can be calculated by ProteinScape software) and Mascot score (see http://www.matrixscience.com) of the hit found by MS/MS or MS (indicated by *) searches. Sequence coverage is calculated from the peptide mass fingerprint (PMF) identification, when present (see Table S1). In cases in which the same protein was identified by both means, the higher score is reported. Scores falling above the significance threshold for the respective database and search type are printed in bold black type. In the case of searches of the National Center for Biotechnology Information non-redundant (NCBInr) database, scores for fungal hits falling below the 95% significance threshold for the entire database, but above the significance threshold for a search of fungal proteins, are printed in normal black type. Subsignificant scores are indicated by grey background. For significance thresholds, see Supplement S3. The identification for spot 98 was viewed as significant because it was the top scoring hit of both the PMF and MS/MS searches, although both scores were subthreshold.

et al., 2005; Noir *et al.*, 2005), can be considered as mobile protein factories that are 'ready to start' on physical contact with a suitable (host) surface. This map provides a basis for the comparative proteomic analysis of further developmental phases of these obligate biotrophic phytopathogens. The proteomic features specific to the feeding organs (haustoria), in particular, promise to be a rich source of information on the biotrophic lifestyle.

EXPERIMENTAL PROCEDURES

Growth conditions of plants and fungi

Barley (*Hordeum vulgare*, I10, a near-isogenic line of cultivar Ingrid containing the *Mla12* resistance gene) plants were grown from seed in a controlled environment at 17 °C, with a 16-h light/8-h dark cycle. Plants were inoculated at the age of 7 days by

dusting fresh conidia from infected plants with sporulating *Blumeria graminis* f.sp. *hordei* (race K1). Conidia for proteomic analysis were collected from sporulating colonies at 7 days post-inoculation using a customized vacuum system (adapted from Johnson-Brousseau and McCormick, 2004), and stored at –80 °C until protein extraction.

Protein extraction and purification

Bgh conidia (approximately 600 mg/replicate) were ground in liquid nitrogen and a small amount of sand using a mortar and pestle. The fine powder was suspended in 1 mL of extraction buffer [50 mM Tris-Base pH 8.0; 10 mM ethylenediaminetetraacetic acid (EDTA); 0.5% 3-[(3-cholamidopropyl)dimethylammonio]-1-propanesulphonate (CHAPS); 10 mM dithiothreitol (DTT); one protease inhibitor cocktail tablet (Roche, Mannheim, Germany)]. Extraction was performed by subjecting the sample to five repetitions of vortexing (30 s each), interrupted by short pauses on ice (30 s each). After centrifugation at 16 000 ***g*** for 5 min at 4 °C, the supernatant was removed and stored on ice. From the remaining pellet, the extraction procedure was repeated with 500 μL of extraction buffer, and the supernatants were pooled. The protein concentration of the supernatant was determined by the Bradford assay with bovine serum albumin as the standard. From the supernatants, the proteins were precipitated with one volume of 10% trichloroacetic acid in acetone overnight at –20 °C. After centrifugation at 10 000 ***g*** for 15 min at 4 °C, the supernatant was discarded and the pellet was washed with chilled 90% acetone. Residual liquid was removed and, after drying on ice, the crude extract was stored at –80 °C until electrophoretic analysis. Before loading for isoelectric focusing (IEF), the crude protein pellet was solubilized in 0.7 mL of dense sodium dodecylsulphate (SDS) buffer [0.1 M pH 8.0 Tris-HCl; 30% (w/v) sucrose; 2% (w/v) SDS; 5% (v/v) 2-mercaptoethanol]. Then, 0.7 mL of Tris-buffered phenol pH 8.0 (Biomol, Hamburg, Germany) was added, and the resulting mixture was vortexed for 30 s. After centrifugation, the phenol phase was collected and five volumes of chilled 0.1 M ammonium acetate in methanol were added. Samples were kept overnight at –20 °C for precipitation. After centrifugation, the pellet was washed twice with chilled 0.1 M ammonium acetate in methanol and twice with 80% (v/v) acetone.

Two-dimensional gel electrophoresis

Two-dimensional polyacrylamide gel electrophoresis was performed using the NuPAGE ZOOM Benchtop Proteomics system (Invitrogen, Carlsbad, CA, USA). Proteins (160 μg) were solubilized in 160 μL of sample rehydration buffer [7 M urea; 2 M thiourea; 2% CHAPS; 0.5% ZOOM Carrier Ampholytes pH 3–10 (Invitrogen); 20 mM DTT; 0.1% bromophenol blue]. Prior to IEF, ZOOM strips (length, 7.7 cm) pI 3–10 non-linear, pI 4–7 linear and pI 6–10 linear (Invitrogen) were incubated for 16 h in the rehydration solution containing the sample; IEF was conducted using the following step gradient: 0–175 V (1 min), 175 V (15 min), 175–2000 V (45 min), 2000 V (25 min). After IEF, the strips used for gel electrophoresis were first equilibrated in 4.5 mL of lithium dodecylsulphate (LDS) sample buffer, together with 0.5 mL of 10 × sample reducing agent (Invitrogen), and subsequently in the same solution containing 125 mM iodoacetamide without reducing agent (15 min each). The samples were separated in the second dimension on NuPAGE Novex 4%–12% Bis-Tris ZOOM gels (8 cm × 8 cm) in 2-(*N*-morpholino)ethanesulphonic acid (MES)-SDS running buffer (Invitrogen), and the proteins were stained with colloidal Coomassie blue using PageBlue (Fermentas, Vilnius, Lithuania).

In-gel digestion and MS

After two-dimensional gel electrophoresis, spots of various intensities were visually selected, robotically picked (PROTEINEERsp, Bruker Daltonics, Bremen, Germany) and tryptically digested in gel (PROTEINEERdp, Bruker Daltonics). Aliquots of the digests were automatically spotted onto AnchorChip targets (Bruker Daltonics) in a thin-layer preparation with α-cyano-4-hydroxy-cinnamic acid for subsequent MALDI-TOF analysis, according to Gobom *et al.* (2001). The mass spectra of tryptic peptides were acquired with a Bruker Daltonics Ultraflex III MALDI-TOF/TOF spectrometer (for instrument parameters, see Supplement S2 in 'Supporting Information'). The resulting PMFs were processed in FlexAnalysis 3.0 (Bruker Daltonics) and used to identify the corresponding proteins in the ProteinScape 1.3 database system (Protagen AG, Bruker Daltonics, Bremen, Germany), which triggered Mascot (Matrix Science Ltd., London, UK) searches.

All samples were then recrystallized on the target by the addition of 1 μL of recrystallization solution (ethanol, acetone and 0.1% trifluoroacetic acid in a 6 : 3 : 1 ratio) and subjected to MALDI-TOF/TOF analysis. LIFT MS/MS spectra (Suckau *et al.*, 2003) were collected for selected precursors according to the following policy: when a protein was identified from the PMF (Mascot score exceeding 95% probability threshold), two assigned peptides of sufficient strength were fragmented for verification and three unassigned peptides were fragmented for further elucidation; when initial searches indicated multiple proteins, the precursor selection was altered by hand to try to verify all initial hypothetical identifications; when initial searches yielded no hits to the PMFs, five precursors were selected on the basis of signal quality alone.

Database searching

MS and MS/MS data were used to screen the NCBInr database (version 2007_12–26) (http://www.ncbi.nlm.nih.gov/entrez/

query.fcgi?db=Protein). The mass spectral data were also searched against *Bgh* ESTs in all six reading frames (NCBI EST status as of 5 February 2008) and against translated ORFs generated from the current (assembly June 2007) *Bgh* draft genome sequence (P. Spanu and coworkers, unpublished data; http://www.blugen.org/). Scores exceeding the Mascot 95% probability limit or the peptide identity threshold for the respective database are presented in boldface black type. Scores exceeding the 95% threshold for fungal protein searches are printed in normal black type. When identified by both MS and MS/MS data, the higher Mascot score is presented in Table 1. A complete listing of all scores and matching peptide sequences is provided in Table S1, and a listing of the Mascot significance thresholds for the various databases is listed in Supplement S3 (see 'Supporting Information'). Sequence coverage was computed from the PMF match, when present. Matches obtained only through MS/MS searches have a correspondingly low coverage. No sequence coverage was computed for EST matches as these do not correspond to full-size proteins.

When identified from ESTs or *Bgh* ORFs, BLAST searches were performed to obtain a match to a full-length protein; then, the predicted pI and molecular mass (MM) were determined using the Expasy Compute pI/Mw tool (http://expasy.org/tools/pi_tool.html). For protein accessions identified directly, these values were calculated by ProteinScape software (Bruker Daltonics).

Functional categories were assigned according to the PANTHER (*P*rotein *AN*alysis *TH*rough *E*volutionary *R*elationships) classification system (http://www.pantherdb.org/), and refined by hand when necessary.

ACKNOWLEDGEMENTS

We thank Cristina Micali for collecting the *Bgh* spores, Ursula Wienecke for excellent technical assistance, and Sarah Maria Schmidt and Elmon Schmelzer for providing the scanning electron micrographs shown in Fig. 1. Research in the lab of R.P. is supported by grants of the Max-Planck Society and the Deutsche Forschungsgemeinschaft (DFG).

REFERENCES

Both, M. and Spanu, P.D. (2004) *Blumeria graminis* f.sp. *hordei*, an obligate pathogen of barley. In: *Plant–Pathogen Interactions* (Talbot, N., ed.), pp. 202–218. Oxford: Blackwell Publishing.

Both, M., Csukai, M., Stumpf, M.P.H. and Spanu, P.D. (2005a) Gene expression profiles of *Blumeria graminis* indicate dynamic changes to primary metabolism during development of an obligate biotrophic pathogen. *Plant Cell*, **17**, 2107–2122.

Both, M., Eckert, S.E., Csukai, M., Muller, E., Dimopoulos, G. and Spanu, P.D. (2005b) Transcript profiles of *Blumeria graminis* development during infection reveal a cluster of genes that are potential virulence determinants. *Mol. Plant–Microbe Interact.* **18**, 125–133.

Braun, U., Cook, R.T.A., Inman, A.J. and Shin, H.D. (2002) The taxonomy of the powdery mildew fungi. In: *The Powdery Mildews* (Bélanger, R.R., Bushnell, W.R., Dik, A.J. and Carver, L.W., eds), pp. 13–55. St Paul, MN: APS Press.

Collins, N.C., Sadanandom, A. and Schulze-Lefert, P. (2002) Genes and molecular mechanisms controlling powdery mildew resistance in barley. In: *The Powdery Mildews* (Bélanger, R.R., Bushnell, W.R., Dik, A.J. and Carver, L.W., eds), pp. 134–145. St Paul, MM: APS Press.

Cooper, B., Garrett, W.M. and Campbell, K.B. (2006) Shotgun identification of proteins from uredospores of the bean rust *Uromyces appendiculatus*. *Proteomics*, **6**, 2477–2484.

Cooper, B., Neelan, A., Campbell, K., Lee, J., Liu, G., Garrett, W.M., Scheffler, B.E. and Tucker, M.L. (2007) Protein accumulation changes associated with germination of the *Uromyces appendiculatus* uredospore. *Mol. Plant–Microbe Interact.* **20**, 857–866.

Gobom, J., Schuerenberg, M., Mueller, M., Theiss, D., Lehrach, H. and Nordhoff, E. (2001) Cyano-4-hydroxycinnamic acid affinity sample preparation. A protocol for MALDI-MS peptide analysis in proteomics. *Anal. Chem.* **73**, 434–438.

Green, J.R., Carver, T.L.W. and Gurr, S.J. (2002) The formation and function of infection and feeding structures. In: *The Powdery Mildews* (Bélanger, R.R., Bushnell, W.R., Dik, A.J. and Carver, L.W., eds), pp. 66–82. St Paul, MN: APS Press.

Hernández, R., Cesar, C., Diez-Orejas, R. and Gil, C. (2004) Two-dimensional reference map of *Candida albicans* hyphal forms. *Proteomics*, **4**, 374–382.

Holmes-Davis, R., Tanaka, C.K., Vensel, W.H., Hurkman, W.J. and McCormick, S. (2005) Proteome mapping of mature pollen of *Arabidopsis thaliana*. *Proteomics*, **5**, 4864–4884.

Hückelhoven, R. and Kogel, K.H. (2003) Reactive oxygen intermediates in plant–microbe interactions: who is who in powdery mildew resistance? *Planta*, **216**, 891–902.

Johnson-Brousseau, S.A. and McCormick, S. (2004) A compendium of methods useful for characterizing *Arabidopsis* pollen mutants and gametophytically-expressed genes. *Plant J.* **39**, 761–775.

Kim, Y., Nandakumar, M.P. and Marten, M.R. (2007) Proteomics of filamentous fungi. *Trends Biotechnol.* **25**, 395–400.

McKeen, W.E. (1970) Lipid in *Erysiphe graminis hordei* and its possible role during germination. *Can J. Microbiol.* **16**, 1041–1044.

Mi, H., Guo, N., Kejariwal, A. and Thomas, P.D. (2007) PANTHER version 6: protein sequence and function evolution data with expanded representation of biological pathways. *Nucleic Acids Res.* **35**, 247–252.

Noir, S., Brautigam, A., Colby, T., Schmidt, J. and Panstruga, R. (2005) A reference map of the *Arabidopsis thaliana* mature pollen proteome. *Biochem. Biophys. Res. Commun.* **337**, 1257–1266.

Osherov, N. and May, G.S. (2001) The molecular mechanisms of conidial germination. *FEMS Microbiol. Lett.* **199**, 153–160.

Rampitsch, C., Bykova, N.V., McCallum, B.D., Beimcik, E. and Ens, W. (2006) Analysis of the wheat and *Puccinia triticina* (leaf rust) proteomes during a susceptible host–pathogen interaction. *Proteomics*, **6**, 1897–1907.

Seong, K.-Y., Zhao, X., Xu, J.-R., Güldener, U. and Kistler, H.C. (2008) Conidial germination in the filamentous fungus *Fusarium graminearum*. *Fungal Genet. Biol.* **45**, 389–399.

Suckau, D., Resemann, A., Schuerenberg, M., Hufnagel, P., Franzen, J. and Holle, A. (2003) A novel MALDI LIFT-TOF/TOF mass spectrometer for proteomics. *Anal. Bioanal. Chem.* **376**, 952–965.

Thomas, P.D., Campbell, M.J., Kejariwal, A., Mi, H., Karlak, B., Daverman, R., Diemer, K., Muruganujan, A. and Narechania, A. (2003) PANTHER: a library of protein families and subfamilies indexed by function. *Genome Res.* **13**, 2129–2141.

Yin, Z., Stead, D., Selway, L., Walker, J., Riba-Garcia, I., McInerney, T., Gaskell, S., Oliver, S.G., Cash, P. and Brown, A.J.P. (2004) Proteomic response to amino acid starvation in *Candida albicans* and *Saccharomyces cerevisiae*. *Proteomics*, **4**, 2425–2436.

Zhang, Z., Henderson, C. and Gurr, S.J. (2004) *Blumeria graminis* secretes an extracellular catalase during infection of barley: potential role in suppression of host defence. *Mol. Plant Pathol.* **5**, 537–547.

Zhang, Z., Henderson, C., Perfect, E., Carver, T.L.W., Thomas, B.J., Skamnioti, P. and Gurr, S.J. (2005) Of genes and genomes, needles and haystacks: *Blumeria graminis* and functionality. *Mol. Plant Pathol.* **6**, 561–575.

SUPPORTING INFORMATION

Additional Supporting Information may be found in the online version of this article:

Supplement S1 FASTA file of polypeptides derived from the *Blumeria graminis* f.sp. *hordei* (*Bgh*) genome sequence. The conceptual translation relates to the BluGen *Bgh* genome assembly from June 2007 (P. Spanu and coworkers, unpublished data; http://www.blugen.org/).

Supplement S2 Instrument parameters. Additional parameters for mass spectrometry (MS) and LIFT MS/MS data acquisition with a Bruker Daltonics UltraflexIII (Suckau *et al.*, 2003).

Supplement S3 Significance thresholds. Mascot score thresholds for significant identifications for peptide mass fingerprint (PMF) and tandem mass spectrometry (MS/MS) searches of the various sequence resources used in this study.

Table S1 Detailed mass spectrometry (MS) results. Expanded representation of MS and MS/MS database search results, including peptide mass fingerprint (PMF) match scores, MS/MS match scores and matching peptide sequences.

Table S1 Explanatory remarks for Table S1.

Please note: Wiley-Blackwell are not responsible for the content or functionality of any supporting materials supplied by the authors. Any queries (other than missing material) should be directed to the corresponding author for the article.